Frontiers of Physics
https://doi.org/10.1007/s11467-019-0920-5
Front. Phys.
14(6), 63602 (2019)

RESEARCH ARTICLE

Evidence of anisotropic Landau level splitting in topological semimetal ZrSiS under high magnetic fields

Jun-Ran Zhang†, Bo Liu, Ming Gao, Yong-Bing Xu‡, Rong Zhang

Jiangsu Provincial Key Laboratory of Advanced Photonic and Electronic Materials, Collaborative Innovation Center of Advanced Microstructures, School of Electronic Science and Engineering, Nanjing University, Nanjing 210023*, China*
Corresponding authors. E-mail: †junran117@163.com; ‡yongbing.xuyork@gmail.com, ybxu@nju.edu.cn
Received May 22, 2019; accepted July 22, 2019

Magneto-transport study has been performed in topological semimetal ZrSiS single crystals under high pulsed magnetic fields. Obvious dependence of Landau level splitting on temperature and angular was investigated. The strong three-dimensional anisotropic nature of Landau level splitting under high pulsed magnetic fields was revealed by the angular dependent measurements, in which the orbital contribution is more dominant than Zeeman splitting. Our studies provide more insights into the physical properties of topological semimetals ZrSiS and shed light on future spintronic applications of ZrSiS.

Keywords topological semimetal, Landau level splitting, high magnetic field

1 Introduction

Topological semimetals viewed as three-dimensional (3D) analogs of graphene have attracted intensive studies in recent years [1–3]. As an emerging quantum states of matter that possess linear band dispersion in the bulk along all three momentum directions, topological semimetals have diverse novel properties, such as ultra-high mobility in Cd_3As_2 [4], extremely large and unsaturated positive magnetoresistance under high pulsed magnetic field in WTe_2 [5] and ZrSiS [6, 7], induced superconductivity by application of high pressure in WTe_2 [8, 9], new type of quantum Hall effect based on Weyl orbits in nanostructures of the 3D topological semimetal Cd_3As_2 [3], and so on. Because of these excellent quantum properties, topological semimetals could act as potential candidates in spintronic applications, such as magnetic sensor [1].

Among the reported topological semimetals, ZrSiS and its family materials have been observed to have other distinct properties. For example, layered crystal structure of ZrSiS is formed from the stack of S-Zr-Si-Zr-S sandwich [10, 11]. One type of Dirac cone in ZrSiS is near the Fermi level and another type is protected by nonsymmorphic symmetry demonstrated by angle-resolved photoemission spectroscopy (ARPES) [10, 12]. ZrSiS has multiple Fermi surface pockets and quasi-2D Dirac Fermi surfaces [7, 10, 13]. The topological phase of ZrSiS can be controlled from nontrivial to trivial by altering angles [14]. The thermoelectric power is an extremely sensitive probe of multiple quantum oscillations that are visible in ZrSiS at temperatures as high as 100 K [15]. All of above-mentioned distinct properties make ZrSiS an amazing topological semimetal, and deserve more studies to dig further physical mechanism.

Landau level splitting gives rise to Shubnikov-de Haas (SdH) oscillations in the longitudinal resistance. Minima in the longitudinal resistance occurs at magnetic field values, at which the magnetic field-dependent density of states at the Fermi level exhibits a minimum [16]. At large enough magnetic fields, the density of states can become zero, which in turn results in zero longitudinal resistance and the well-known quantized and universal values of the Hall voltage [17]. In topological semimetals, obvious Landau level splitting was observed in Cd_3As_2 under high magnetic field, suggesting the removal of spin degeneracy by breaking time reversal symmetry. The results also demonstrated a feasible path to generate a Weyl semimetal phase from Dirac phase by breaking time reversal symmetry [18]. As one of Dirac materials, graphene also shows a phenomenon of Landau splitting under high magnetic field with the zero Landau level splitting into four sublevels, lifting spin and sublattice degeneracy. This phenomenon potentially indicates a many-body correlation in zero Landau level [19]. Clear Landau level splitting can also be observed in a layered antiferromagnet $EuMnBi_2$, which primarily origins from spin depending on the field-tunable magnetic order of Eu moments [20]. Landau level splitting in a two-dimensional electron gas (2DEG) is also as a hallmark of high quality 2DEGs confined in semiconductor heterostructures [16].

In our previous work, splitting of SdH patterns was mentioned briefly [7, 21]. In this study, however, we performed systematic magneto-transport studies of high-

quality ZrSiS single crystals under high pulsed magnetic field and the detailed discussions about Landau level splitting were shown. The well-resolved Landau level splitting at high field was investigated. SdH oscillations clearly demonstrate strong Landau level splitting at pulsed magnetic fields. The spacing of the split Landau levels, defined as the spatial difference of the split peaks, changes with the field direction, revealing a contribution of both the orbital and Zeeman splitting.

2 Experimental details

The ZrSiS single crystals studied in this work were grown by the chemical vapor transport method. The details of sample growth are described in our previous works [7, 21]. Single crystal X-ray diffraction (XRD) (Ultima III Rigaku X-ray diffractometer, Cu-K_α radiation) with 2θ scanned from 10°–55° was employed to investigate growth orientation of the fresh cleavage crystals. To investigate the magneto-transport properties of ZrSiS crystals, Hall-bar and four-terminal devices were fabricated with gold wires attached by silver paint, as schematically shown in the Fig. 1(a). Subsequently, the low-field transport properties were measured using a physical property measurement system (PPMS-9T, Quantum Design). The high-field measurements were performed in a pulsed magnetic field (up to 60 T) at Wuhan National High Magnetic Field Center, China. A constant current was applied within the {001} atomic planes while the magnetic field was changed from perpendicular to parallel to the {001} planes, as depicted by the green arrow.

3 Results and discussion

The crystal of ZrSiS has PbFCl-type structure with tetragonal $P4/nmm$ space group (No. 129) [11]. The tetragonal structure of ZrSiS is formed from a stack of S-Zr-Si-Zr-S sandwich layers [10, 11]. As shown in Fig. 1(b), the reflections in the XRD patterns of the maximum exposed surface of ZrSiS can be indexed as (001). The yellow lines are from PDF 85-0660#. It suggests that the exposed surface of ZrSiS crystals is defined as c-plane. In addition, the values of full-width at half maximum (FWHM) of (002), (003) and (004) peaks are all smaller than 0.09°, suggesting the high crystalline quality of grown ZrSiS. Other structure characterizations can be found at our previous work to reveal the high quality of our sample [7, 21]. Figure 1(c) shows the temperature dependence of longitudinal resistivity ρ_{xx} at zero magnetic field. The ρ_{xx}–T curve describes a typical metallic behavior of ZrSiS due to the semimetal band structure. ZrSiS as a semimetal has an extremely low resistivity at room temperature. To the best of

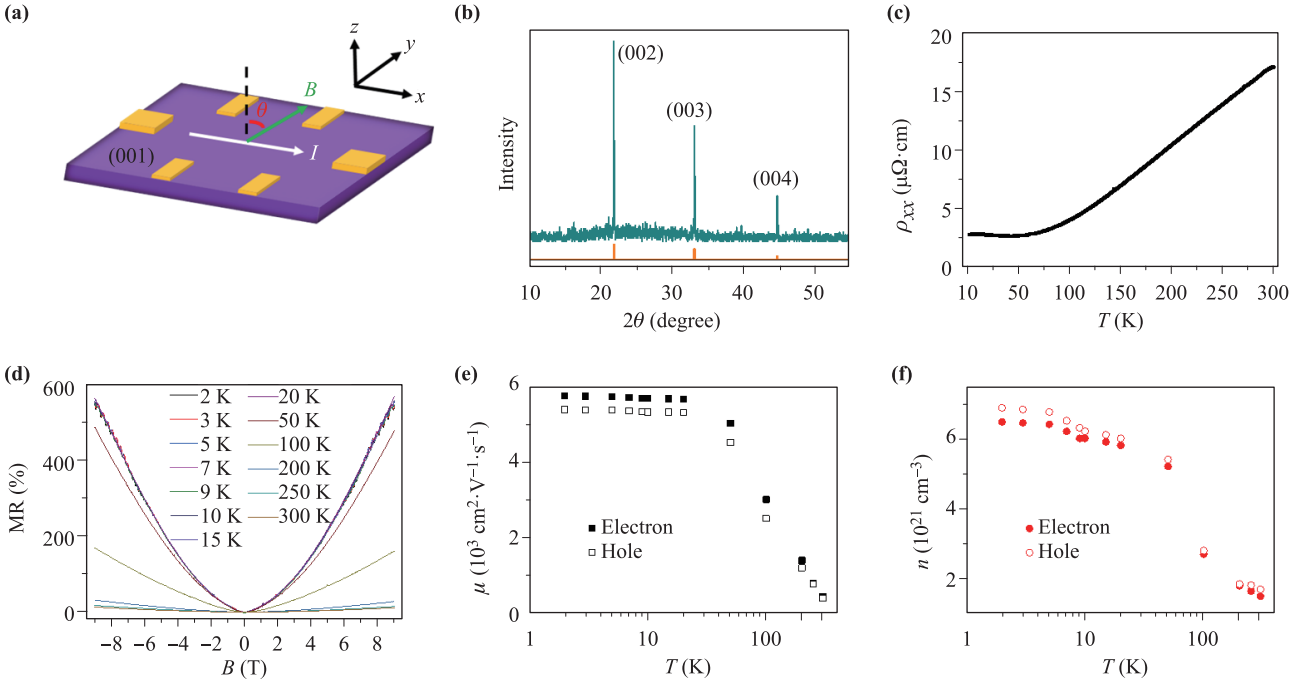

Fig. 1 **(a)** Schematic diagram of our device, a constant current was applied with the {001} atomic planes while the magnetic field was titled in the x–z plane, as depicted by the green arrow. **(b)** X-ray diffraction patterns of the single crystal ZrSiS. The peak position shows that the sample surface is in {001} planes, the yellow lines are from PDF 85-0660#. **(c)** The longitudinal resistivity ρ_{xx} as a function of temperature, showing a typical metallic behavior. **(d)** The longitudinal magnetoresistance at different temperature at $\theta = 0°$. The critical temperature is found to be 50 K, above which the oscillation is not observable. **(e)** The temperature-dependent mobility from 2 K to 300 K. **(f)** The temperature-dependent carrier density from 2 K to 300 K.

our knowledge, ZrSiS has the lowest resistivity of any sulfide known [14]. Figure 1(d) shows the magnetic field dependence of MR at different temperatures. Obvious SdH oscillations can be observed. The critical temperature is 50 K, above which the oscillations disappear. We will not go into details about quantum SdH oscillations here as it has been reported in our previous work [7, 21]. One of the most fascinating features of ZrSiS is the compensated electrons and holes, which resulting extremely large MR [22]. Figures 1(e) and (f) respectively show mobilities and carrier densities of electrons and holes at different temperatures. The almost equal mobility and carrier densities of electrons and holes at different temperatures reveal the electron-hole compensation. The significant enhancement of the mobility can be attributed to the alleviated phonon scattering at very low temperatures [18].

To search the possible novel exotic magneto-transport properties including symmetry breaking, it is necessary to apply higher magnetic fields to excite the lower Landau levels, as shown in Fig. 2(a), where the longitudinal resistivity is plotted against the magnetic field (up to 60 T) at different temperatures. More obvious SdH oscillations can be seen than in Fig. 1(d). Here we use half integers to denote peaks and integers to represent valleys [7]. The Landau level index $n = 3$ can be clearly observed under about 58 T. As expected, lower Landau level can be seen. The obvious Landau level splitting can be clearly witnessed at almost Landau levels under high magnetic field. Figure 2(b) shows the fast Fourier transform (FFT) of the SdH oscillations at various different temperatures. α denotes peak at 65 T, β denotes peak at 411.7 T and γ denotes peak at 693.4 T. The peaks of 2α, 3α, 4α, $\beta + 2\alpha$, and $\beta+6\alpha$ harmonics are all visible. So many frequencies from FFT of ZrSiS may be ascribed to the high pulsed magnetic field, which is also reported in other paper [23]. The areas of the Fermi surface S_F and vector k_F are calculated with the results listed in Table 1. Figure 2(c) shows SdH oscillations under different temperatures after subtracting background signals. Both stronger oscillations and clearer Landau level splitting can be witnessed. As we can see, the splitting-induced double-peak structure gradually evolves into a single peak as the temperature increases from 1.5 to 10 K. This reflects the smearing out of the splitting by the increasing thermal energy at higher temperatures. It has been reported that both Zeeman and orbital contribute to the exchange splitting induced by a magnetic field [24, 25]. In addition, the strong Zeeman splitting at low magnetic fields probed by de Hass–van Alphen quantum oscillations has been observed in ZrSiS [26]. Zeeman splitting also can be observed in topological semimetal $ZrTe_5$ at magnetic field as low as 3 T owing to the large g factor [27]. Zeeman contribution mainly depends on the magnitude of the field and is isotropic with respect to the field direction, while the orbital contribution relies on the shape of the band structure and diminishes away from Dirac point [25].

Table 1 Estimated parameters from the SdH oscillations.

Frenquency No.	F_{SdH} (T)	S_{F} (10^{-3} Å^{-2})	k_{F} (Å^{-1})
α	65.0	6.20	0.044
β	411.7	39.3	0.112
γ	693.4	66.6	0.145

For the sake of the dominant contribution between Zeeman and orbital, the Landau level splitting was investigated as a function of angular at 4.2 K. Figure 3(a) shows the magnetic-field-dependent resistivity at different θ under a high field (up to 60 T). The measurement temperature is at 4.2 K. The obvious angular dependence on SdH oscillations and Landau level splitting are observed. In order to understand the Landau level splitting dependence better in ZrSiS, the resistivity dependence on $1/B\cos\theta$ was plotted after subtracting a smooth background as shown in Fig. 3(b). As we can see from the picture, the peak of Landau level 3.5 splits from one peak to two peaks, and the distance of the two peaks increases as the angular decreases. To better understand the Landau level splitting with changing the angular, we plot the distance between 3.5+ and 3.5− as a function of angular as shown in Fig. 3(c), where $\Delta_{3.5} = 1/B_{3.5-}\cos\theta - 1/B_{3.5+}\cos\theta$. A strong angular dependence of is clearly observed, which

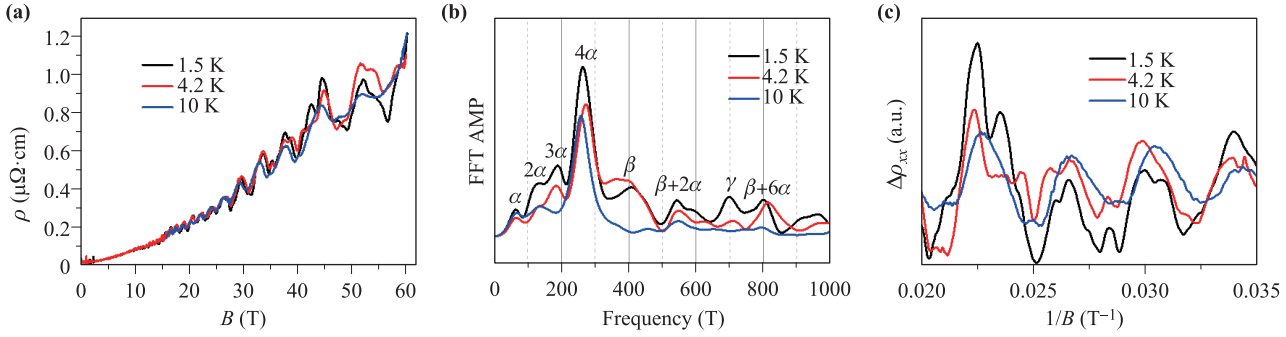

Fig. 2 **(a)** The longitudinal resistivity as a function of high magnetic field up to 60 T at different temperature. **(b)** The corresponding FFT of (a), where 8 peaks can be identified. AMP in the figure means the amplitude. **(c)** The oscillating MR at different temperatures, revealing the energy splitting.

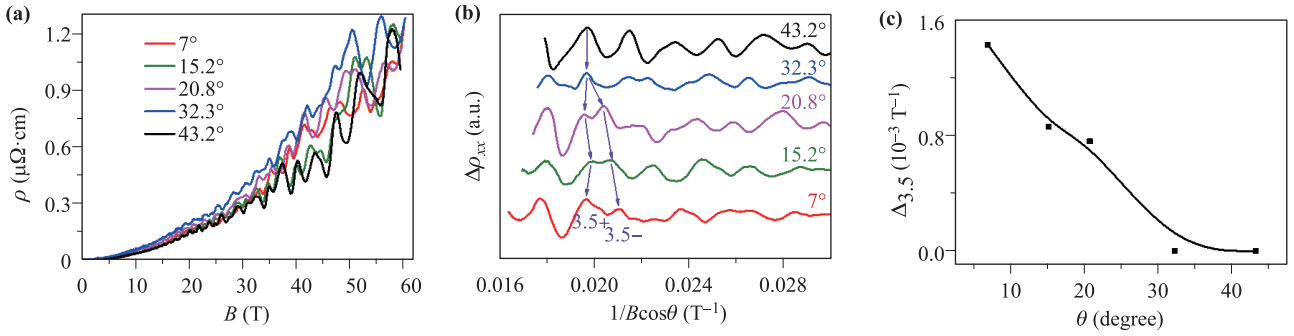

Fig. 3 **(a)** Magnetic-field-dependent resistivity measured at different θ under a high field (up to 60 T) at 2 K. **(b)** The angular dependence of longitudinal resistivity at 4.2 K. The SdH oscillations are observed at different angles. **(c)** The distance between 3.5+ and 3.5− as a function of angular extracted from (b).

indicates that dominated contribution to Landau level is anisotropic orbital splitting rather than the isotropic Zeeman splitting as discussed in the last paragraph [25]. This can be the evidence of anisotropic Landau level splitting in topological semimetal ZrSiS under high magnetic field. In fact, similar splitting of Landau level governed by orbital contribution has been also reported in other topological semimetal materials, such as Cd_3As_2 [18, 25]. It has been reported by Cao *et al.* that the split spacing for the 2.5^{th} peak shows less angular dependence than that for the 3^{rd} and the 3.5^{th} peaks. This suggests that the Zeeman term presumably dominates in the 2.5^{th} peak splitting while for the 3^{rd} and the 3.5^{th} peaks the orbital term has a large contribution [18]. The results reported by Cao *et al.* show that different Landau level splitting may origin from different contribution of Zeeman or orbital. In addition, the angular dependence of Landau level splitting also reveals the three-dimensional (3D) character of ZrSiS. The 3D nature of ZrSiS has also been evidenced by direct quantum transport study in our previous work [21].

4 Conclusions

In summary, we report the observation of Landau level splitting under high magnetic field up to 60 T in topological nodal-line semimetal ZrSiS single crystals. The orbital-dependent Landau level splitting can be significantly affected by the direction of magnetic field. The discussions of Landau level splitting in ZrSiS single crystals provide a better understanding of the physical nature of topological nodal-line semimetal, which would determine the potential device applications in the near future.

Acknowledgements This work was supported by the National Key Research and Development Program of China (Grant No. 2016YFA0300803), the National Natural Science Foundation of China (Grant Nos. 61427812, 11774160, 11574137, 11874203, 61822403, and U1732159), and the Fundamental Research Funds for the Central Universities (Grant No. 021014380080). The authors also would like to thank the supports from the Collaborative Innovation Center of Solid State Lighting and Energy-saving Electronics and the Program for High-level Entrepreneurial and Innovative Talent Introduction, Jiangsu Province.

References

1. N. P. Armitage, E. J. Mele, and A. Vishwanath, Weyl and Dirac semimetals in three-dimensional solids, *Rev. Mod. Phys.* 90(1), 015001 (2018)
2. J. Xiong, S. K. Kushwaha, T. Liang, J. W. Krizan, M. Hirschberger, W. Wang, R. Cava, and N. Ong, Evidence for the chiral anomaly in the Dirac semimetal Na_3Bi, *Science* 350(6259), 413 (2015)
3. C. Zhang, Y. Zhang, X. Yuan, S. Lu, J. Zhang, A. Narayan, Y. Liu, H. Zhang, Z. Ni, R. Liu, E. S. Choi, A. Suslov, S. Sanvito, L. Pi, H. Z. Lu, A. C. Potter, and F. Xiu, Quantum Hall effect based on Weyl orbits in Cd_3As_2, *Nature* 565(7739), 331 (2019)
4. M. Neupane, S. Y. Xu, R. Sankar, N. Alidoust, G. Bian, C. Liu, I. Belopolski, T. R. Chang, H. T. Jeng, H. Lin, A. Bansil, F. Chou, and M. Z. Hasan, Observation of a three-dimensional topological Dirac semimetal phase in high-mobility Cd_3As_2, *Nat. Commun.* 5(1), 3786 (2014)
5. M. N. Ali, J. Xiong, S. Flynn, J. Tao, Q. D. Gibson, L. M. Schoop, T. Liang, N. Haldolaarachchige, M. Hirschberger, N. P. Ong, and R. J. Cava, Large, non-saturating magnetoresistance in WTe_2, *Nature* 514(7521), 205 (2014)
6. R. Singha, A. K. Pariari, B. Satpati, and P. Mandal, Large nonsaturating magnetoresistance and signature of nondegenerate Dirac nodes in ZrSiS, *Proc. Natl. Acad. Sci. USA* 114(10), 2468 (2017)
7. X. Wang, X. Pan, M. Gao, J. Yu, J. Jiang, J. Zhang, H. Zuo, M. Zhang, Z. Wei, W. Niu, Z. Xia, X. Wan, Y. Chen, F. Song, Y. Xu, B. Wang, G. Wang, and R. Zhang, Evidence of both surface and bulk Dirac bands and anisotropic nonsaturating magnetoresistance in ZrSiS, *Adv. Electron. Mater.* 2(10), 1600228 (2016)
8. D. Kang, Y. Zhou, W. Yi, C. Yang, J. Guo, Y. Shi, S. Zhang, Z. Wang, C. Zhang, S. Jiang, A. Li, K. Yang, Q. Wu, G. Zhang, L. Sun, and Z. Zhao, Superconductivity

emerging from a suppressed large magnetoresistant state in tungsten ditelluride, *Nat. Commun.* 6(1), 7804 (2015)

9. X. C. Pan, X. Chen, H. Liu, Y. Feng, Z. Wei, Y. Zhou, Z. Chi, L. Pi, F. Yen, F. Song, X. Wan, Z. Yang, B. Wang, G. Wang, and Y. Zhang, Pressure-driven dome-shaped superconductivity and electronic structural evolution in tungsten ditelluride, *Nat. Commun.* 6(1), 7805 (2015)
10. L. M. Schoop, M. N. Ali, C. Strasser, A. Topp, A. Varykhalov, D. Marchenko, V. Duppel, S. S. Parkin, B. V. Lotsch, and C. R. Ast, Dirac cone protected by non-symmorphic symmetry and three-dimensional Dirac line node in ZrSiS, *Nat. Commun.* 7(1), 11696 (2016)
11. Q. Xu, Z. Song, S. Nie, H. Weng, Z. Fang, and X. Dai, Two-dimensional oxide topological insulator with iron-pnictide superconductor LiFeAs structure, *Phys. Rev. B* 92(20), 205310 (2015)
12. A. Topp, J. M. Lippmann, A. Varykhalov, V. Duppel, B. V. Lotsch, C. R. Ast, and L. M. Schoop, Non-symmorphic band degeneracy at the Fermi level in ZrSiTe, *New J. Phys.* 18(12), 125014 (2016)
13. M. Neupane, I. Belopolski, M. M. Hosen, D. S. Sanchez, R. Sankar, M. Szlawska, S. Y. Xu, K. Dimitri, N. Dhakal, P. Maldonado, P. M. Oppeneer, D. Kaczorowski, F. Chou, M. Z. Hasan, and T. Durakiewicz, Observation of topological nodal fermion semimetal phase in ZrSiS, *Phys. Rev. B* 93(20), 201104 (2016)
14. M. N. Ali, L. M. Schoop, C. Garg, J. M. Lippmann, E. Lara, B. Lotsch, and S. S. Parkin, Butterfly magnetoresistance, quasi-2D Dirac Fermi surface and topological phase transition in ZrSiS, *Sci. Adv.* 2(12), e1601742 (2016)
15. M. Matusiak, J. R. Cooper, and D. Kaczorowski, Thermoelectric quantum oscillations in ZrSiS, *Nat. Commun.* 8(1), 15219 (2017)
16. S. Schmult, V. V. Solovyev, S. Wirth, A. Großer, T. Mikolajick, and I. V. Kukushkin, Magneto-optical confirmation of Landau level splitting in a GaN/AlGaN 2DEG grown on bulk GaN, *J. Vac. Sci. Technol. B* 37(2), 021210 (2019)
17. K. Klitzing, G. Dorda, and M. Pepper, New method for high-accuracy determination of the fine-structure constant based on quantized Hall resistance, *Phys. Rev. Lett.* 45(6), 494 (1980)
18. J. Cao, S. Liang, C. Zhang, Y. Liu, J. Huang, Z. Jin, Z. G. Chen, Z. Wang, Q. Wang, J. Zhao, S. Li, X. Dai, J. Zou, Z. Xia, L. Li, and F. Xiu, Landau level splitting in Cd_3As_2 under high magnetic fields, *Nat. Commun.* 6(1), 7779 (2015)
19. Y. Zhang, Z. Jiang, J. P. Small, M. S. Purewal, Y. W. Tan, M. Fazlollahi, J. D. Chudow, J. A. Jaszczak, H. L. Stormer, and P. Kim, Landau-level splitting in graphene in high magnetic fields, *Phys. Rev. Lett.* 96(13), 136806 (2006)
20. H. Masuda, H. Sakai, M. Tokunaga, M. Ochi, H. Takahashi, K. Akiba, A. Miyake, K. Kuroki, Y. Tokura, and S. Ishiwata, Impact of antiferromagnetic order on Landau-level splitting of quasi-two-dimensional Dirac fermions in $EuMnBi_2$, *Phys. Rev. B* 98(16), 161108(R) (2018)
21. J. Zhang, M. Gao, J. Zhang, X. Wang, X. Zhang, M. Zhang, W. Niu, R. Zhang, and Y. Xu, Transport evidence of 3D topological nodal-line semimetal phase in ZrSiS, *Front. Phys.* 13(1), 137201 (2018)
22. Y. Y. Lv, B. B. Zhang, X. Li, S. H. Yao, Y. Chen, J. Zhou, S. T. Zhang, M. H. Lu, and Y. F. Chen, Extremely large and significantly anisotropic magnetoresistance in ZrSiS single crystals, *Appl. Phys. Lett.* 108(24), 244101 (2016)
23. S. Pezzini, M. R. van Delft, L. M. Schoop, B. V. Lotsch, A. Carrington, M. I. Katsnelson, N. E. Hussey, and S. Wiedmann, Unconventional mass enhancement around the Dirac nodal loop in ZrSiS, *Nat. Phys.* 14(2), 178 (2018)
24. Z. Wang, Y. Sun, X. Q. Chen, C. Franchini, G. Xu, H. Weng, X. Dai, and Z. Fang, Dirac semimetal and topological phase transitions in A_3Bi (A = Na, K, Rb), *Phys. Rev. B* 85(19), 195320 (2012)
25. S. Jeon, B. B. Zhou, A. Gyenis, B. E. Feldman, I. Kimchi, A. C. Potter, Q. D. Gibson, R. J. Cava, A. Vishwanath, and A. Yazdani, Landau quantization and quasiparticle interference in the three-dimensional Dirac semimetal Cd_3As_2, *Nat. Mater.* 13(9), 851 (2014)
26. J. Hu, Z. Tang, J. Liu, Y. Zhu, J. Wei, and Z. Mao, Nearly massless Dirac fermions and strong Zeeman splitting in the nodal-line semimetal ZrSiS probed by de Haas–van Alphen quantum oscillations, *Phys. Rev. B* 96(4), 045127 (2017)
27. Y. Liu, X. Yuan, C. Zhang, Z. Jin, A. Narayan, C. Luo, Z. Chen, L. Yang, J. Zou, X. Wu, S. Sanvito, Z. Xia, L. Li, Z. Wang, and F. Xiu, Zeeman splitting and dynamical mass generation in Dirac semimetal $ZrTe_5$, *Nat. Commun.* 7(1), 12516 (2016)